Crystallography-Driven Positive Exchange Bias in Co/CoO Bilayers

A. K. Suszka,[1,*] O. Idigoras,[1] E. Nikulina,[1] A. Chuvilin,[1,2] and A. Berger[1]

[1]*CIC nanoGUNE Consolider, E-20018 Donostia-San Sebastian, Spain*

[2]*IKERBASQUE, Basque Foundation for Science, 48011, Bilbao, Spain*

(Received 30 March 2012; published 23 October 2012)

We have studied the temperature dependence of the exchange bias effect in epitaxial Co/CoO bilayer structures with in-plane uniaxial magnetocrystalline anisotropy. We have measured the anisotropic positive exchange bias, which is independent from the initial cooling field value. Synchronous with the occurrence of positive exchange bias, distinct changes in the magnetization reversal process indicate a temperature-dependent rotation of the effective anisotropy and exchange bias axis. Model calculations based upon the electron microscopy-determined epitaxial Co/CoO-interface structure corroborate this interpretation.

DOI: 10.1103/PhysRevLett.109.177205 PACS numbers: 75.70.Cn, 75.50.Ee

Exchange bias arises due to the interfacial exchange coupling between ferromagnets (FM) and antiferromagnets (AFM) and it is usually "set" by cooling FM-AFM systems in the presence of a magnetic field below the antiferromagetic ordering temperature (Néel temperature) [1]. The most profound consequence of the microscopic interfacial exchange coupling is a shift of the FM hysteresis loop along the axis of the magnetic field. Interestingly, this shift can be either opposing or following the direction of the initial field cooling (FC), which leads to the observation of so-called negative or positive exchange bias field (H_{bias}). Hereby, $H_{\text{bias}} = (H_{cL} + H_{cR})/2$ with H_{cL} and H_{cR} being the left and right coercive fields, respectively. Positive H_{bias} is rarely observed as it indicates a stabilization of the FM orientation against the direct Zeeman energy term acting on the FM system component [2–5]. Two well-understood cases of positive H_{bias} have been previously observed [6–8]. In FM/FeF_2 systems, positive H_{bias} arises from the antiferromagnetic coupling of interfacial FM-AFM spins in combination with a Zeeman energy-induced magnetic ordering of the AFM spins. Anomalous positive H_{bias} also originates from an "artificial" shift of the coercivity, which has been recently observed in patterned FM-AFM systems with uniaxial magnetic anisotropy [8]. In this case, the macroscopic appearance of positive H_{bias} is related to the asymmetric magnetization reversal so that H_{bias} does not actually follow the orientation of the local exchange coupling field H_{ex} acting on the FM as part of the overall microscopic energy of the system [9,10].

In this Letter we study the temperature-dependent interplay of magnetic anisotropy and exchange bias for epitaxial [(100)Co/(110)CoO]-bilayer films. The positive H_{bias} that is observed in an intermediate temperature range is independent from the FC strength and thus cannot be explained in terms of a competition between bulk and interface magnetic ordering in the AFM. Instead, the positive H_{bias} depends strongly on the direction of FC relative to the easy axis (EA) of magnetization in our uniaxial Co-thin films.

Our samples were deposited by dc sputtering onto hydrofluoric-etched Si(110) substrates. The deposition sequence was Si substrate/Ag75.0/Cr50.0/Co9.0/CoO2.0. Thicknesses are defined in nm, and CoO was formed by natural oxidation of Co under controlled conditions. The buffer layers of Ag and Cr create a template for growth of highly ordered (100) hcp Co films with in-plane c-axis orientation, which is the magnetically easy axis of hcp Co [11]. A detailed description of the epitaxial growth procedure has been reported elsewhere [12,13]. The structural analysis of our Co/CoO bilayer was carried out using a Titan G2 60–300 transmission electron microscope (TEM) (FEI, Netherlands). Hysteresis loops were measured using a Quantum Design vibrating sample magnetometer after first warming the samples up to 350 K, i.e., well above the bulk Néel temperature of CoO ($T_N = 293$ K) and subsequent cool down to 5 K in the presence of a magnetic field applied either along [001] or along [$\bar{1}$20] crystallographic directions of Co, which are the magnetic EA and hard axis (HA), respectively.

The often-complex exchange bias phenomenon requires an in-depth knowledge of the structural properties of the studied system. Therefore, we have performed a detailed structural analysis of the studied samples using high-resolution TEM (HRTEM). Figure 1(a) shows a HRTEM cross-section image of one of our Co/CoO samples with hcp Co and rocksalt CoO lattice structures. Figures 1(d) and 1(e) are the corresponding Fourier transform (FT) patterns, which identify the [111] crystallographic zone axis of CoO and the [021] zone axis of Co. Figure 1(b) shows a color-coded "dark field" image reconstructed from the FT data by using the reflections that are marked in Fig. 1(e). It confirms that the reflections colored in red [($\bar{2}$20), ($\bar{2}$02), and (0$\bar{2}$2)] correspond to a continuous and epitaxial 2 nm thick layer of CoO on top of Co, visible in the upper part of Fig. 1(b). Figures 1(c) and 1(f) show the

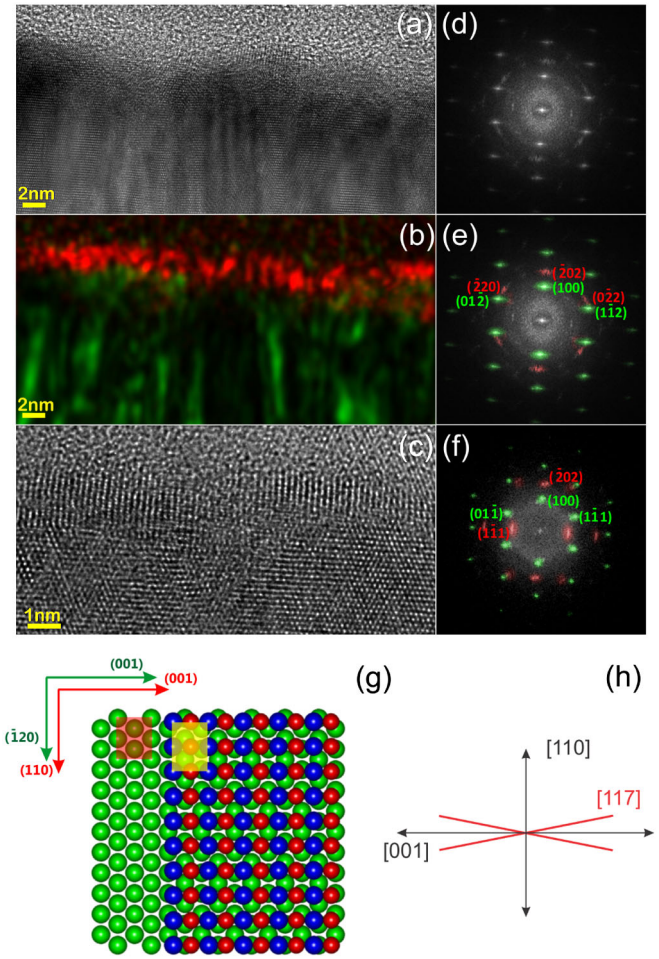

FIG. 1 (color online). (a),(c) HRTEM images of a cross section of the epitaxial Co/CoO stack and corresponding FTs (d)–(f). Cross section (c) is rotated by 20° with respect to (a). (b) Color-coded "dark field" image reconstructed from FT (e). (g) Top view of a model of the Co/CoO interface of our sample. (h) Schematic view of $(110)_{CoO}$, with $\langle 117 \rangle$ easy spin axes of bulk CoO.

same sample tilted by approximately 20°, with CoO oriented along the [121] zone axis and Co along the [011] zone axis. The combination of Figs. 1(e) and 1(f) results in the determination of the epitaxial relationship in our samples: $\{110\}_{CoO}\|\{100\}_{Co}$ (interfacial planes), $\{001\}_{CoO}\|\{001\}_{Co}$, and $\{110\}_{CoO}\|\{\bar{1}20\}_{Co}$. Figure 1(g) shows a schematic top view of our Co/CoO interface structure and Fig. 1(h) illustrates the bulk $(110)_{CoO}$ plane, for which the easy spin orientations of bulk CoO along the $\langle 117 \rangle$ directions are marked by red lines [14–16].

Figures 2(a) and 2(b) show H_{bias} as a function of temperature measured along the HA and EA of Co, respectively, for FC values equal to 2.5, 30.0, and 50.0 kOe [17]. Along the HA [Fig. 2(a)], we observe after the initial field cooldown the expected negative H_{bias} for low temperatures, which strongly decays with increasing temperature for all FC values. This decay is a commonly observed

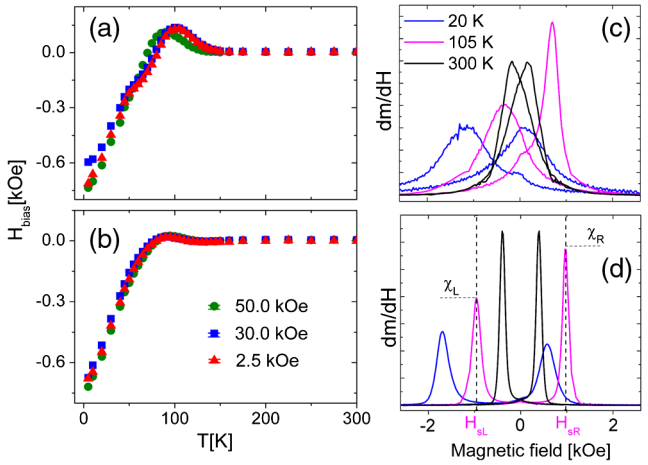

FIG. 2 (color online). H_{bias} versus temperature curves for HA (a) and EA (b) measurements. The applied FC values and representative measurement error bars are shown in the legend. (c), (d) dm/dH curves extracted from hysteresis loops for HA and EA, respectively. The values of left and right switching fields (H_{sL} and H_{sR}) and left and right dm/dH peak heights (χ_L and χ_R) are indicated.

feature in exchange-biased systems. Instead of simply vanishing, H_{bias} changes its sign at approximately 80 K, which leads to the observation of positive H_{bias} reaching a peak value at 100 K. A further increase of the temperature results in the disappearance of H_{bias} at the apparent blocking temperature: $T_{B(HA)} = 160$ K. Similarly, the EA field-cooling procedure [Fig. 2(b)] also leads to the initial low temperature observation of negative H_{bias} which decays with increasing temperature, changes its sign at approximately 80 K, and subsequently vanishes at an approximate blocking temperature: $T_{B(EA)} = 120$K.

As Fig. 2 also reveals, the values of positive H_{bias} and T_B do not change significantly for different values of the FC. This behavior is different from the one observed in FM/FeF_2 systems and eliminates the possibility of a Zeeman energy-induced sign reversal of exchange bias. Also, it is clear from the data that the positive H_{bias} is anisotropic and seems to be sensitive only to the FC direction with respect to the EA of Co. The peak value of positive $H_{bias} = 130$ Oe along the HA is substantially higher than along the EA, where it reaches a peak of only $H_{bias} = 20$ Oe. Previous experimental observations of positive H_{bias} in Co/CoO have reported only very small values, which are similar to our EA measurement [18–21].

In order to understand the transition from negative to positive H_{bias} we have analyzed the magnetization reversal curves in more detail. Specifically, we have determined $dm/dH(H)$ via numerical differentiation. Figures 2(c) and 2(d) show dm/dH curves for selected temperatures after the HA and EA 2.5 kOe FC procedure, respectively. The curves illustrate examples of the negative H_{bias} (20 K), positive H_{bias} (105 K), and no exchange bias states (300 K). All dm/dH curves show two distinct peaks,

in which the left peak relates to the descending and right peak to the ascending branch of the hysteresis loop. The central positions of left and right dm/dH peaks, H_{sL}, and H_{sR}, correspond to the steepest slope of the hysteresis loop and can be associated with the switching fields of the magnetic system in reference to the Stoner-Wohlfarth model. The heights of right and left dm/dH peaks are indicated as χ_R and χ_L, respectively, in Fig. 2(d). The $T = 20$ K dm/dH curve measured along the HA [Fig. 2(c)] shows the expected shift of H_{sL} towards negative magnetic fields associated with negative H_{bias}. The HA curve measured at 105 K shows a shift of H_{sR} towards positive magnetic field as well as a significant asymmetry of the peak heights, while the 300 K dm/dH curves are both symmetric and centered around zero magnetic field. The EA dm/dH curves [Fig. 2(d)] behave very similarly, except for the fact that the peaks are narrower and that at low temperatures a peak height asymmetry is visible that is opposite of the positive H_{bias} behavior. The shift of H_{sR} and the overall asymmetry of the curves at 105 K are synchronous with the appearance of positive H_{bias}. Detailed temperature-dependent H_{sR} and H_{sL} data are shown in Figs. 3(a) and 3(b) for the HA and EA cases, in comparison to the measured coercivities H_{cR} and H_{cL}. For the HA, H_{sL} and H_{cL} overlap up to approximately 130 K, at which point they split and remain separated up to room temperature. H_{sR} and H_{cR} overlap up to approximately 80 K, but are separated for all higher temperatures. Within the Stoner-Wohlfarth model, coercive and switching fields overlap for hysteresis loops measured in proximity to the EA, while they separate in the vicinity of the HA [22]. Thus the low temperature HA hysteresis loop shape imitates a near easy axis–like magnetization reversal, and upon transitioning from negative to positive H_{bias}, the HA hysteresis transforms to exhibit the shape of hard axis–like switching up to room temperature.

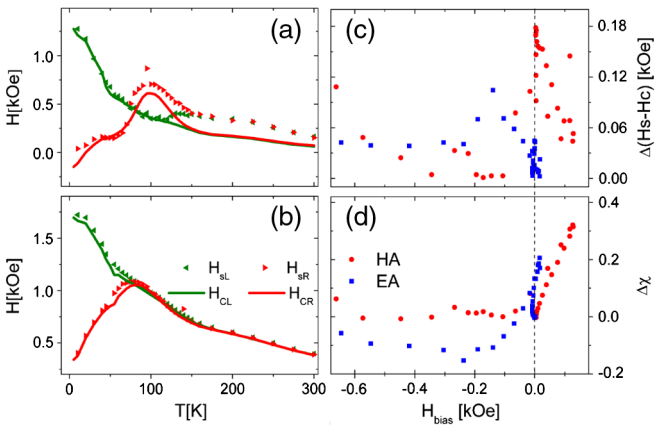

FIG. 3 (color online). Absolute values of H_{sL}, H_{sR} (points) and H_{cL} and H_{cR} (lines) along the HA (a) and EA (b). (c) $\Delta(H_s - H_c)$ as a function of H_{bias} for the HA (circles) and EA (squares), (d) $\Delta\chi(H)$ versus H_{bias} in the case of HA and EA; the dashed lines mark $H_{\text{bias}} = 0$ in (c) and (d).

In the case of the EA, we do not observe any significant detachment of H_s and H_c in the entire temperature range for either branch of the hysteresis loop. Thus, the most profound difference between the EA and HA behavior occurs in proximity to the appearance of positive H_{bias} values, which are also found to be far larger in the HA direction. Figure 3(c) shows the average difference between the switching fields and the respective coercivities: $\Delta(H_s - H_c) = [(H_{sL} - H_{cL}) + (H_{sR} - H_{cR})]/2$, for the HA and EA measurements as a function of H_{bias} measured after 2.5 kOe FC. In the case of the HA, two regimes are evident: the region of negative H_{bias}, where $\Delta(H_s - H_c)$ is small and vanishes within the precision of our measurement, and the region of positive H_{bias}, where $\Delta(H_s - H_c)$ significantly increases and stays at elevated levels even for $T > 160$ K, where no exchange bias is visible anymore. The clear shift of $\Delta(H_s - H_c)(H_{\text{bias}})$ away from zero in the HA measurements occurs simultaneously with the transition from negative to positive H_{bias}. In the case of the EA measurements there seems to be no significant change of $\Delta(H_s - H_c)$ over the whole H_{bias} range.

Figure 3(d) shows the normalized difference between the heights of the right and left dm/dH peaks: $\Delta\chi(H) = (\chi_R - \chi_L)/(\chi_R + \chi_L)$ as a function of H_{bias} for the HA (squares) and the EA (circles) measurements. In the case of the HA, nearly no peak asymmetry is present for all negative values of H_{bias}, while a significant asymmetry arises for positive H_{bias}. This asymmetry indicates more abrupt magnetization reversal for the ascending branch in comparison to the descending branch of the hysteresis loop, a behavior that exhibits its peak effect at the highest value of H_{bias}. In the case of the EA, $\Delta\chi(H)$ indicates a more abrupt switching of the descending branch of the hysteresis loop in comparison to the ascending branch for negative H_{bias}. Upon reaching positive H_{bias}, $\Delta\chi(H)$ changes its sign and also here reaches its maximum value synchronously with maximum positive H_{bias}.

The results of Fig. 3(d) indicate that in both cases, EA and HA, the exchange coupling to the AFM not only causes a temperature-dependent size change and sign reversal of H_{bias}, but also changes the reversal mechanism exactly and the point of transition from negative to positive H_{bias}. Thus, the temperature dependence of the microscopically acting H_{ex} cannot be limited to a simple change in amplitude, but must also undergo a reorientation with increasing temperature. Furthermore, the data of Fig. 3(c) indicate that for the HA case the effective magnetically hard axis also reorients as a function of temperature from an effective direction away from the nominal HA to a direction much closer to it. Given that the crystallographic EA of magnetization does not change as a function of temperature, this change must originate from an exchange-bias-induced uniaxial anisotropy caused by the CoO [23,24].

To mimic this behavior and investigate the appearance of positive H_{bias}, we have calculated hysteresis loops for

arbitrary orientations of in-plane easy axis and exchange bias field orientation using the free energy equation:

$$f = M_s H\cos(\theta) - M_s H_{ex}\cos(\theta - \theta_{ex}) - K_U\cos^2(\theta - \theta_U), \quad (1)$$

where H and M_s are externally applied magnetic field and saturation magnetization, H_{ex} and K_U are the microscopic exchange bias field and the effective uniaxial magnetic anisotropy constant, while θ, θ_{ex}, and θ_U are the angles of magnetization, exchange bias, and uniaxial anisotropy axis with respect to the applied magnetic field direction [8]. Figure 4(a) shows a map representation of H_{bias} (θ_{ex}, θ_U) for $(M_s H_{ex})/K_U = 0.1$, a ratio we would expect to occur close to T_B. The map shows two pronounced regions of θ_{ex} and θ_U, in which positive H_{bias} appears: one close to the HA for negative θ_{ex} and one in a broader range for positive θ_{ex} values. Even though by increasing the $(M_s H_{ex})/K_U$ ratio the relative size and location of these positive H_{bias} islands changes slightly [25], they do not move towards $\theta_{ex} = 0$ or change their general shape in a very substantial manner, so that we can discuss the temperature-dependent behavior of our samples with the aid of only one map.

The temperature-dependent evolution of our system along the θ_U axis is rather straightforward. For the EA measurements, the system will be near $\theta_U = 0$ in the entire temperature range, while the data in Figs. 3(a) and 3(c) show that for the HA oriented measurements, θ_U must be substantially lower than 90° at low temperatures and will increase to $\theta_U = 90°$ as the temperature increases. The temperature-dependent evolution of θ_{ex}, whose existence is shown by the data in Fig. 3(d) for both EA and HA measurements, is not easy to determine exactly, but one can make some reasonable assumptions. Given the large negative H_{bias} values, i.e., the effective implementation of exchange bias, at low temperatures and the rather small reversal asymmetry, it is reasonable to assume that the effective θ_{ex} is small, i.e., $\theta_{ex} \approx 0$. The driving force to cause deviations from $\theta_{ex} = 0$, and thus the temperature-dependent reorientation of the local exchange field, must be related to the energetics and preferred spin order state of the CoO layer. While the direction of the spin moments in CoO-thin film can differ from the bulk magnetic structure [26], experimental sensitivity limitations did not allow us to determine the AFM spin structure and its temperature dependence for our Co/CoO-bilayer system. For this reason we make the assumption that the CoO in our films has the bulk spin order as its lowest energy state, which is schematically shown in Figs. 4(b) and 4(c) for the HA and EA cases, respectively. Furthermore, we assume for simplicity that it is the volume averaged spin orientation of the CoO that determines the direction of the microscopic exchange bias, i.e., θ_{ex}. The easy spin directions for bulk CoO points along the $\langle 117\rangle$ directions, which are present in the film plane and encompass an angle of 79° with the $[110]_{CoO}$ and 11° with the $[001]_{CoO}$. So, under the assumption of the CoO-bulk spin structure being the primary cause for the temperature-dependent exchange field reorientation, one would expect θ_{ex} to change by 79° in the HA case, and by only 11° in the EA case.

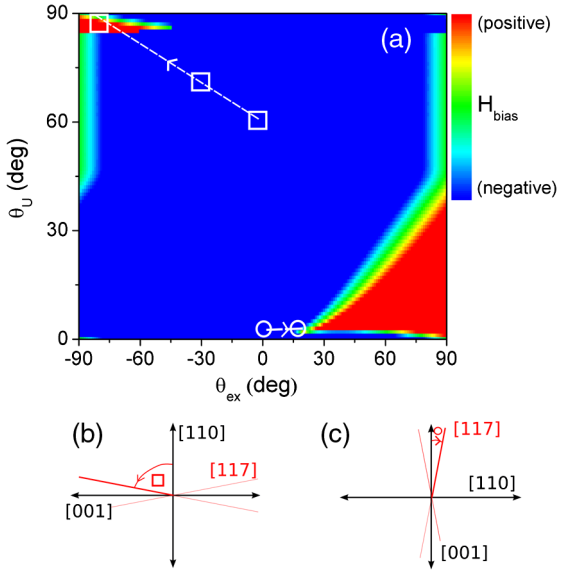

FIG. 4 (color online). (a) H_{bias} as a function of θ_{ex} and θ_U shown as a color-coded map. The lines indicate the possible temperature evolution of our Co/CoO-bilayer system for the EA (circle) and HA (square) cases. (b), (c) Schematic illustrations of rotation of the exchange bias axis away from the FC direction towards the $\langle 117\rangle_{CoO}$ axis in both cases.

Based upon these considerations, we have drawn schematically the possible temperature evolution of the effective (θ_{ex}, θ_U) location for our Co/CoO-bilayer system for both the HA and the EA case [27]. For the EA direction the (θ_{ex}, θ_U) point moves rather little and only tangentially touches the major island of positive exchange bias stability. Thus, one would expect from Fig. 4(a) that positive H_{bias} in the EA direction is rather weak. This is indeed our experimental observation. On the other hand, the (θ_{ex}, θ_U) point describing the HA system shows a very substantial movement as a function of temperature. Here, the exchange bias axis orientation θ_{ex} shows an extensive temperature-dependent movement, which is also expected for θ_U due to the existence of an exchange-bias-induced uniaxial energy term [28]. Correspondingly, the HA (θ_{ex}, θ_U) trajectory completely crosses the upper island of positive H_{bias} and thus makes this effect much more pronounced along the HA, which is exactly what we find experimentally. So, the simple model of Eq. (1) explains, at least qualitatively, the anisotropic positive H_{bias} behavior that we observe in our epitaxial Co/CoO bilayers and identifies the sample crystallography as the driving force for it.

We acknowledge Axel Hoffmann and Igor Roshchin for their valuable comments and discussion. We acknowledge funding from the Basque Government under Programs No. PI2009-17 and under the Etortek Program

nanoIKER'11, Contracts No. IE11-304 and No. BFI09.284, and the Spanish Ministry of Science and Education under Project No. MAT2009-07980. E. N acknowledges financial support from FEI Company (Netherlands).

*Corresponding author.
a.suszka@nanogune.eu

[1] W. H. Meiklejohn and C. P. Bean, Phys. Rev. **105**, 904 (1957).
[2] P. D. Kulkarni, A. Thamizhavel, V. C. Rakhecha, A. K. Nigam, P. L. Paulose, S. Ramakrishanan, and A. K. Grover, Europhys. Lett. **86**, 47 003 (2009).
[3] R. P. Singh, C. V. Tomy, and A. K. Grover, Appl. Phys. Lett. **97**, 182505 (2010).
[4] S. R. Ali, M. B. Janjua, M. Fecioru-Morariu, D. Lott, C. J. P. Smits, and G. Güntherodt, Phys. Rev. B **82**, 020402(R) (2010).
[5] H. Shi, D. Lederman, N. R. Dilley, R. C. Black, J. Diedrichs, K. Jensen, and M. B. Simmonds, J. Appl. Phys. **93**, 8600 (2003).
[6] J. Nogués, D. Lederman, T. J. Moran, and I. K. Schuller, Phys. Rev. Lett. **76**, 4624 (1996).
[7] H. Ohldag, H. Shi, E. Arenholz, J. Stöhr, and D. Lederman, Phys. Rev. Lett. **96**, 027203 (2006).
[8] S. H. Chung, A. Hoffmann, and M. Grimsditch, Phys. Rev. B **71**, 214430 (2005).
[9] O. Hovorka, A. Berger, and G. Friedman, J. Appl. Phys. **101**, 09E515 (2007).
[10] O. Hovorka, A. Berger, and G. Friedman, Appl. Phys. Lett. **89**, 142513 (2006).
[11] W. Yang, D. N. Lambeth, and D. E. Laughlin, J. Appl. Phys. **85**, 4723 (1999); H. Gong, W. Yang, M. Rao, D. E. Laughlin, and D. N. Lambeth, Mater. Res. Soc. Symp. Proc. **562**, 27 (1999).
[12] O. Idigoras, A. K. Suszka, P. Vavassori, P. Landeros, J. M. Porro, and A. Berger, Phys. Rev. B **84**, 132403 (2011).
[13] O. Idigoras, P. Vavassori, J. M. Porro, and A. Berger, J. Magn. Magn. Mater. **322**, L57 (2010).
[14] S. Maat, K. Takano, S. S. P. Parkin, and E. E. Fullerton, Phys. Rev. Lett. **87**, 087202 (2001).
[15] J. Bransky, I. Bransky, and A. A. Hirsch, J. Appl. Phys. **41**, 183 (1970).
[16] J. H. Greiner, A. E. Berkowitz, and J. E. Weidenborner, J. Appl. Phys. **37**, 2149 (1966).
[17] Prior to any of these measurements, exchange bias training effects were accommodated first by cycling multiple low temperature hysteresis loops at 5 K, to ensure that our temperature-dependent measurements were separated from training effects.
[18] T. Gredig, I. N. Krivotorov, P. Eames, and E. D. Dahlberg, Appl. Phys. Lett. **81**, 1270 (2002).
[19] F. Fettar, L. Cagnon, and N. Rougemaille, Appl. Phys. Lett. **97**, 192502 (2010).
[20] F. Radu, M. Etzkorn, R. Siebrecht, T. Schmitte, K. Westerholt, and H. Zabel, Phys. Rev. B **67**, 134409 (2003).
[21] The exchange bias field effects observed here are substantially larger than the experimental errors, as shown in Fig. 2(b) by the maximum errors in every measurement sequence.
[22] G. Bertotti, *Hysteresis in Magnetism* (Academic, New York, 1998).
[23] M. Grimsditch, A. Hoffmann, P. Vavassori, H. Shi, and D. Lederman, Phys. Rev. Lett. **90**, 257201 (2003).
[24] W. N. Cao, J. Li, G. Chen, J. Zhu, C. R. Hu, and Y. Z. Wu, Appl. Phys. Lett. **98**, 262506 (2011).
[25] While the near HA positive exchange bias island expands somewhat along the θ_U axis upon increasing the $(M_s H_{ex})/K_U$ ratio, the near-EA island decreases in size and shifts towards slightly higher values of θ_U and θ_{ex}.
[26] Y. Ijiri, T. C. Schulthess, J. A. Borchers, P. J. van der Zaag, and R. W. Erwin, Phys. Rev. Lett. **99**, 147201 (2007).
[27] The low temperature HA starting point (θ_{ex}, θ_U) was determined based on the low temperature remanent magnetization ratio between hard and easy axis. To do this accurately the hereby-considered remanence values are not measured at zero external field but at the magnetic field value that compensates for the exchange bias shift of the respective hysteresis loops.
[28] Here, θ_U describes the temperature-dependent orientation of the effective uniaxial anisotropy axis, which is given by the sum of two noncollinear terms: the magnetocrystalline anisotropy of Co and an exchange-bias-induced uniaxial anisotropy, which weakens strongly with increasing temperature.